0273-2289/1559-0291 (Online)/06/135/0159/$30.00

Differential Response Induced by Exposure to Low-Dose Ionizing Radiation in SHSY-5Y and Normal Human Fibroblast Cells

A. McLachlan-Burgess,[1] S. McCarthy,[1] C. Griffin,[1] J. Richer,[2] R. G. Cutler,[3] and S. Pandey*,[1]

[1]Department of Chemistry and Biochemistry, University of Windsor, 401 Sunset Avenue, Windsor, ON, Canada N9B 3P4, E-mail: spandey@uwindsor.ca; [2]Windsor Regional Cancer Centre, Windsor, ON, Canada; and [3]Kronos Science Laboratories, Phoenix, AZ

Received December 20, 2005; Revised February 14, 2006; Accepted February 14, 2006

Abstract

Radiation therapy has been used in the treatment of a wide variety of cancers for nearly a century and is one of the most effective ways to treat cancer. Low-dose ionizing radiation (IR) can interfere with cell division of cancer and normal cells by introducing oxidative stress and injury to DNA. The differences in the response to IR-induced DNA damage and increased reactive oxygen species between normal human fibroblasts (NHFs) and cancerous SHSY-5Y cells were considered. H2AX staining and comet assays revealed that NHF cells responded by initiating a DNA repair sequence whereas SHSY-5Y cells did not. In addition, NHF cells appeared to quench the oxidative stress induced by IR, and after 24 h no DNA damage was present. SHSY-5Y cells, however, did not repair their DNA, did not quench the oxidative stress, and showed characteristic signs that they were beginning to undergo apoptosis. These results indicate that there is a differential response between this cancerous and normal cell line in their ability to respond to low-dose IR, and these differences need to be exploited in order to treat cancer effectively. Further study is needed in order to elucidate the mechanism by which SHSY-5Y cells undergo apoptosis following radiation and why these normal cells are better equipped to deal with IR-induced double-strand breaks and oxidative stress.

Index Entries: Radiation; apoptosis; double-strand breaks; DNA damage; DNA repair.

*Author to whom all correspondence and reprint requests should be addressed.

Introduction

Cancer is one of the largest killers today, despite improved cancer treatments and an increased understanding of the causes of the disease. Approximately 70% of diagnosed cancer patients will receive radiation therapy, whereas only 50% will receive some form of chemotherapy *(1)*. Radiation therapy has been used in the treatment of a wide variety of cancers for nearly a century and is one of the most effective ways to treat cancer *(2)*. In addition, radiation therapy may be combined with other forms of cancer therapy such as chemotherapy or surgery *(2)*.

Radiation therapy functions by focusing a beam of ionizing radiation (IR) on the cancerous growth so that only a specific area is treated and minimal damage is caused to the surrounding healthy tissue *(3)*. IR interferes with the cell division of cancer and normal cells by introducing oxidative stress and injury to DNA *(1)*. This DNA damage can be directly or indirectly induced, and the extent of the damage is often dependent on the dose of radiation *(4)*. IR may be followed by cell-cycle disturbance, irregular mitosis, or cell death, depending on the dose of radiation and the extent of damage to the cell *(4)*. Cancer cells are more susceptible to undergoing cell death following radiation therapy than normal cells *(1)*, but the reason for this remains unknown. Additionally, the differential response of cancer and normal cells to low-dose radiation is unknown.

Apoptosis is known to occur following treatment with radiation in both cancerous and normal cells *(5,6)*. Apoptosis is a form of programmed cell death and consists of a series of nontraumatic and characteristic physiologic changes that quickly lead to the removal of the affected cells by phagocytosis *(7,8)*. Apoptosis can be induced by receptor activation, growth factor deprivation, DNA damage, and oxidative stress *(9)*. There are two main pathways of apoptotic cell death: the death receptor–induced extrinsic pathway and the mitochondria-apoptosome-mediated intrinsic pathway *(10)*.

There are two types of IR-induced apoptosis: premitotic and postmitotic. The type of apoptotic cell death depends on the magnitude of the damage caused by radiation and the magnitude of the radiation itself *(4)*. Premitotic apoptosis, which follows treatment with high doses of radiation, occurs before cell division and is associated with immediate activation of caspase-3 *(4)*. Postmitotic apoptosis follows treatment with low doses of radiation and apoptosis occurs after cells complete one cell division *(4)*. It is still unclear whether or not low-dose radiation induces the intrinsic or extrinsic pathway *(11)*.

DNA double-strand breaks (DSBs) are considered the most significant injury induced by IR *(12–14)* and activate two routes of DNA repair in normal mammalian cells: the homologous-recombination (HR) and nonhomologous end-joining (NHEJ) pathways *(1)*. These pathways are activated by several serine/threonine kinases that work to detect the DSB and signal to the NHEJ pathway *(1,15)*. Three of these kinases, ataxia telangiectasia mutated (ATM), ATM and Rad3-related (ATR), and the

DNA-dependent protein kinase catalytic subunit (DNA-DPKcs), are thought to be responsible for the phosphorylation of serine-139 of H2AX, a histone protein *(16)*. A fluorescent antibody specific for the phosphorylated form of H2AX (γH2AX) can be used to visualize foci produced when DNA repair is initiated *(12)*.

In the present study, the in vitro effect of low-dose radiation on normal human fibroblasts (NHFs) and SHSY-5Y (neuroblastoma) cells was investigated. The differences in the response to DNA damage between the NHF and SHSY-5Y cells were considered with respect to whether cells undergo apoptosis or initiate a DNA repair sequence. The possible mechanism of how low-dose radiation induces apoptosis or DNA repair in cancerous SHSY-5Y and NHF cells is discussed.

Materials and Methods

Cell Culture

Human neuroblastoma (SHSY-5Y) cells (American Type Culture Collection) were grown at 37°C and 5% CO_2 in Ham's F12 medium (Gibco BRL, VWR, Canada) with 2 m*M* L-glutamine (Gibco BRL, VWR) supplemented with 1.5 g/L of sodium carbonate, 10% fetal bovine serum (FBS) (Sigma, Canada) and 10 mg/mL of gentamycin (complete medium) (Gibco BRL, VWR). Human diploid fibroblasts (AG09309) (NHFs) were obtained from Coriell Institute for Medical Research (NJ) and grown in Earle's minimum essential medium supplemented with 15% (v/v) FBS (Sigma), and 2 m*M* L-glutamine (Gibco BRL, VWR) supplemented with 1.5 g/L of sodium carbonate, essential and nonessential amino acids, vitamins, and 10 mg/L of gentamycin (all from Gibco BRL, VWR) in 5% CO_2 in a humid incubator at 37°C.

Radiation Treatment

Forty-eight hours after plating, cells were subjected to 20 mgy of IR at the Windsor Regional Cancer Centre (Windsor, Ontario) using a Gulmay D-3300 Orthovoltage X-ray. Cells were irradiated under normal conditions within Petri plates. Cells were incubated for 1 or 24 h following radiation. After incubation, various experiments were performed in order to evaluate the effect of the radiation on both cell lines. All experiments were performed in triplicate.

Data Analysis

All pictures were processed using Adobe Photoshop 7.0 software. Microsoft Excel 6.0 software was used for data representation and statistical analysis. Statistical significance values were obtained with an analysis of variance (ANOVA) with a 95% confidence level using StatSoft Statistica.

Cellular Staining and Microscopy

To examine morphologic changes, SHSY-5Y and NHF cells were grown and radiated as previously described, followed by staining with Hoechst 33342 at a final concentration of 10 μ*M* (Molecular Probes of Invitrogen, Canada, Burlington, ON, Canada). The cells were examined under a fluorescent microscope (Leica DM IRB, Germany), and phase contrast and fluorescence pictures were taken. In addition, trypan blue (Gibco BRL) staining and hemocytometer counting were used to assess the percentage of viable cells.

H2AX Staining

SHSY-5Y and NHF cells were grown on cover slips in six-well plates and radiated as previously described. The cells were prepared for staining by washing the cover slips with cold phosphate-buffered saline (PBS) and incubating with approx 500 μL of cold 4% paraformaldehyde (PFA) for 10 min at room temperature. PFA was removed and the cover slips were allowed to dry at room temperature for approx 30 min.

H2AX staining was carried out using a combination and adaptation of previously published methods *(17,18)*. The cover slips were washed with PBS three times for 5 min and incubated in 70% ethanol for 5 min at room temperature. Again the cover slips were washed three times with PBS for 5 min. The cover slips were then incubated in 10% FBS in PBS for 1 h at room temperature followed by an additional three washings with PBS for 5 min each. The cover slips were incubated with primary antibody (anti-H2AX) (Upstate USA Inc., Charlottesville, VA) for 1 h at room temperature and washed three times for 5 min with PBS. The cover slips were incubated in secondary antibody (anti-mouse IgG) (Sigma) for 1 h at room temperature and washed with PBS as previously described. The cover slips were then incubated in 1 μL/mL Hoechst 33342 for 5 min at room temperature and washed with PBS as previously. The cover slips were allowed to dry and were mounted on slides. The slides were examined under a Bio-Rad 1024 Confocal Microscope (Bio-Rad, Hercules, CA) and pictures were taken.

Comet Assay

A comet assay was performed using a slight modification of a previously published method *(19)*. As previously described, SHSY-5Y and NHF cells were grown and radiated. After an allotted time, cells were harvested by trypsinization and 10 μL of cell suspension (approx 10,000 cells) was mixed with 80 μL of warm 0.75% low-melting-point agarose (Sigma) at 37°C in a microfuge tube. The mixture was spread on a glass slide that had been precoated with 200 μL of 0.1% agarose (EM Sciences). Spreading was conducted so that half of the gel was on the coarse surface and the other half was on the smooth, transparent surface, because agarose gel tends to slide away from the smooth surface during processing. The slides were incubated at 4°C for 5–10 min. They were then immediately immersed in a tray

containing freshly prepared cold lysis buffer with 2.5 *M* NaCl (BDH, Canada), 100 m*M* Na_2EDTA, 10 m*M* Tris (pH 10.0), 1% Triton X-100, and 10% dimethylsulfoxide and incubated in the dark for 1 h at 4°C. Following incubation, the slides were washed in freshly prepared alkaline electrophoresis buffer with 0.3 *M* NaOH and 1 m*M* Na_2EDTA at pH greater than 13.0. The DNA was electrophoresed at 300 mA (0.8 V/cm), washed twice in a neutralizing buffer (0.4 *M* Tris, pH 7.5), and stained with 10 µ*M* Hoechst 33342. The cells were examined under a fluorescent microscope (Leica DM IRB), and phase contrast and fluorescence pictures were taken.

Measurement of Total Reactive Oxygen Species Generation

After treatment as previously described, the production of total reactive oxygen species (ROS) in the SHSY-5Y and NHF cells was measured with the -permeable dye 2*N*, 7*N*-dichlorofluorescein diacetate (DCFDA) (Molecular Probes) and using a slight modification of a previously published procedure *(20)*. The cells were incubated in 10 µ*M* DCFDA at 37°C for 20 min, and fluorescence was measured at an excitation of 500 nm and an emission of 520 nm using a Spectra Max Gemini XS multiwell plate fluorescence reader (Molecular Devices, Sunnyvale, CA). Protein concentration was measured using Bio-Rad protein assay reagent with bovine serum albumin (BSA) (Sigma) as a standard, and the results were calculated per microgram of protein.

Assays for Activation of Proteases

Proteasome and caspase-3 assays were performed using a previously published method *(19)*. Cytosolic SHSY-5Y and NHF cell lysates were used for the protease assays based on a fluorogenic substrate, which contains a tetrapeptide sequence corresponding to the substrate cleavage site. LLVY-AFC was used for proteasome and DEVD-AFC was used for caspase-3 activity assays according to the manufacturer's protocol (Enzyme System Products). Fluorescence was measured at an excitation of 400 nm and an emission of 505 nm in a 96-well microtiter plate using the Spectra Max Gemini XS reader (Molecular Devices). Caspase-3 and proteasome activities were calculated per microgram of protein. Protein concentration was measured using Bio-Rad protein assay reagent with BSA as a standard.

Mitochondrial Membrane Permeability

Following growth and irradiation of SHSY-5Y and NHF cells, mitochondrial membrane permeability was measured using JC-1 dye (Molecular Probes) according to the manufacturer's protocol and a previously published method *(21)*. The cells were treated with 0.5 µ*M* dye and incubated for 10 min. The same cells were also treated with Hoechst 33342 as described above under "Cellular Staining and Microscopy." The cells were examined under a fluorescent microscope (Leica DM IRB), and pictures were taken.

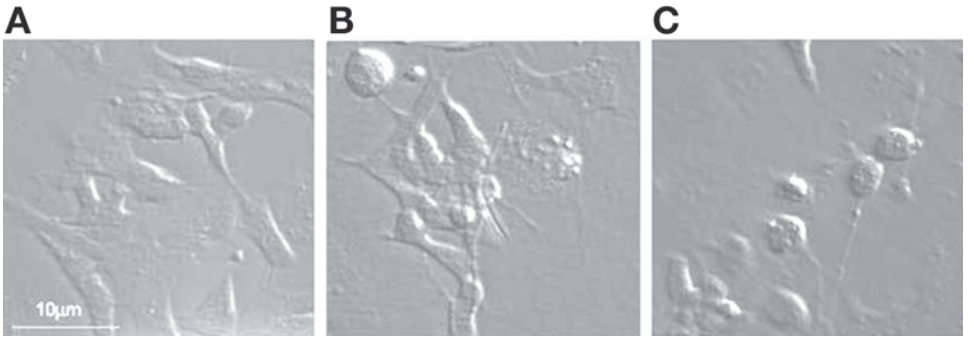

Fig. 1. Morphology of SHSY-5Y cells. SHSY-5Y cells were radiated with 20 mgy of IR as described. Phase contrast pictures were taken **(B)** 1 and **(C)** 24 h after radiation. **(A)** SHSY-5Y cells that were not radiated. Pictures were taken at H400 magnification using a Leica DM IRB microscope. Apoptosis is evident in cells with cellular beading, membrane blebbing, and lifting from the surface.

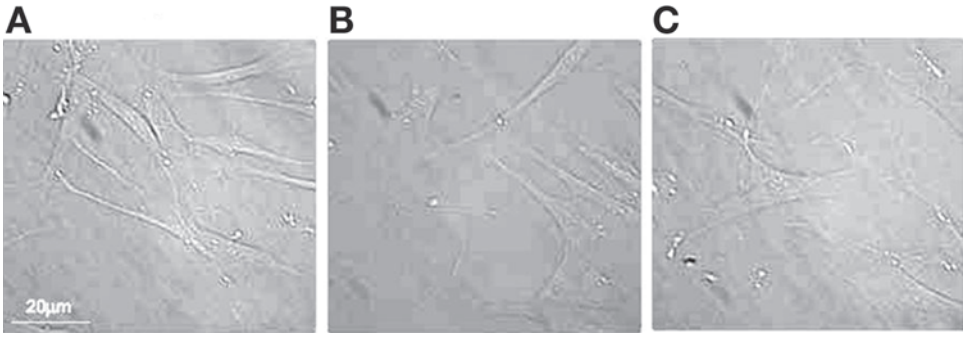

Fig. 2. Morphology of NHF cells. NHF cells were radiated with 20 mgy of IR as described. Phase contrast pictures were taken **(B)** 1 and **(C)** 24 h after radiation. **(A)** NHF cells that were not radiated. Pictures were taken at ×400 magnification using a Leica DM IRB microscope. Apoptosis is evident in cells with cellular beading, membrane blebbing, and lifting from the surface.

Assay for Adenosine Triphosphate

SHSY-5Y and NHF cells were grown and irradiated as previously described and an adenosine triphosphate (ATP) assay was completed. Cytoplasmic cell suspension (100 µL) was incubated with 5 mg/mL of luciferin-luciferase (Sigma), and bioluminescence was measured at 560 nm using the Spectra Max Gemini XS reader. Total cell ATP levels were determined using an assay of internal standards. Protein was estimated using the Bio-Rad protein reagent with BSA as a standard, and the results were calculated per microgram of protein.

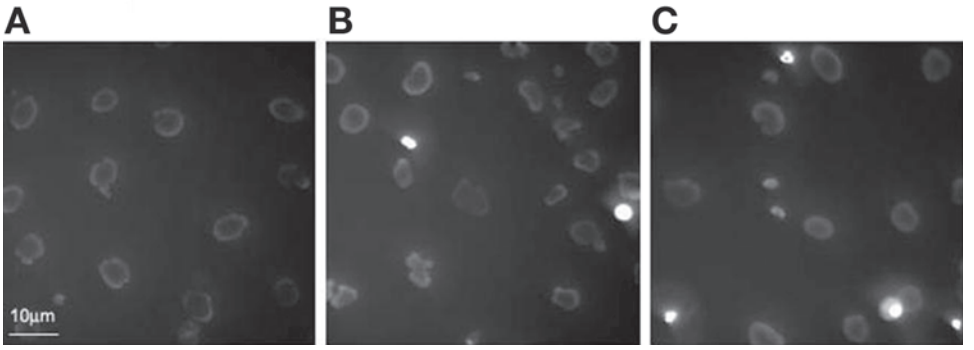

Fig. 3. Nuclear morphology of SHSY-5Y cells. SHSY-5Y cells were radiated with 20 mgy of IR as described. Fluorescent pictures were taken **(B)** 1 and **(C)** 24 h following radiation. **(A)** SHSY-5Y cells that were not radiated. After the allotted time, Hoechst 33342 dye was applied to the cells to examine nuclear morphology. Pictures were taken at ×400 magnification using a Leica DM IRB microscope. Nuclear condensation is evident in cells with bright, condensed, and rounded nuclei.

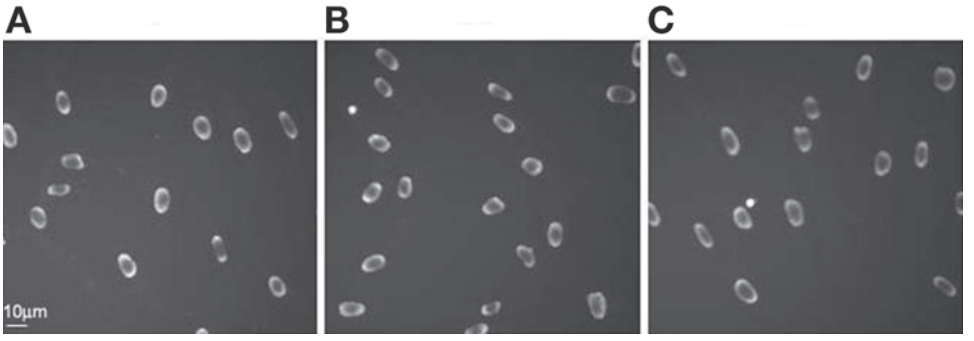

Fig. 4. Nuclear morphology of NHF cells. NHF cells were radiated with 20 mgy of IR as described. Fluorescent pictures were taken **(B)** 1 and **(C)** 24 following radiation. **(A)** NHF cells that were not radiated. After the allotted time, Hoechst 33342 dye was applied to the cells to examine nuclear morphology. Pictures were taken at ×400 magnification using a Leica DM IRB microscope. Nuclear condensation is evident in cells with bright, condensed, and rounded nuclei.

Results

Morphologic Changes Induced by Radiation: Cellular Morphology, Nuclear Morphology, and Trypan Blue Staining in NHF and SHSY-5Y Cells

SHSY-5Y and NHF cells were grown and radiated as previously described and the cellular morphology was observed. Figure 1B shows that 1 h after radiation morphologic changes including beading, membrane blebbing, and lifting from the surface occurred in SHSY-5Y cells, whereas the NHF cells (Fig. 2B) appeared to be the same as the control (Fig. 1A).

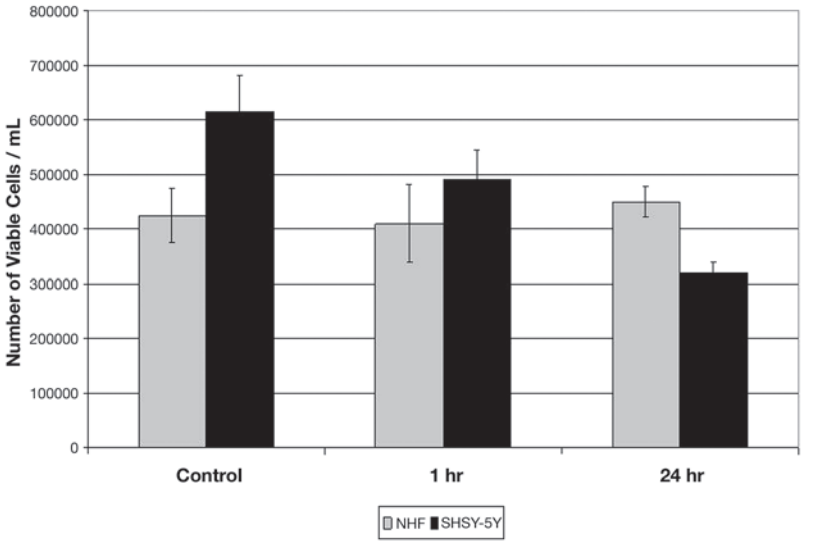

Fig. 5. Trypan blue staining for number of viable cells: NHF and SHSY-5Y. One and 24 h after radiation, trypan blue was used to measure the number of viable NHF (shaded bars) and SHSY-5Y (black bars) cells as previously described. Microsoft Excel Version 6.0 software was used to represent the data and calculate the SD. Results were calculated as the number of viable cells/mL and SEs were calculated using data from three separate sets of experiments.

Twenty-four hours after radiation, SHSY-5Y cells appeared to have a significant increase in the number of morphologic changes (Fig. 1C), whereas NHF cells (Fig. 2C) appeared morphologically similar to control cells (Fig. 2A).

Hoechst staining indicated that 1 h (Fig. 3B) and 24 h (Fig. 3C) after radiation the number of SHSY-5Y cells that had small bright nuclei increased in comparison with control cells (Fig. 3A). The number of NHF cells that had small bright nuclei was similar to that of control cells (Fig. 4A) both 1 h (Fig. 4B) and 24 h (Fig. 4C) after radiation. Nuclear condensation indicated by bright staining was a characteristic feature of apoptosis. These results indicated that SHSY-5Y cells were beginning to show characteristics of apoptosis, whereas NHF cells appeared the same as control.

Trypan blue staining was used to estimate the number of viable cells. The number of viable NHF cells remained approximately the same as that of the control, both 1 and 24 h (Fig. 5) after radiation. One hour after radiation, the number of viable SHSY-5Y cells dropped in comparison with the control, and 24 h after radiation the number of viable cells dropped to almost half (Fig. 5). ANOVA indicated that the control NHF trypan values were not significantly different from 24-h NHF trypan values ($p > 0.05$). ANOVA also indicated that the control SHSY-5Y and 24-h values were significantly different ($p = 0.0083$).

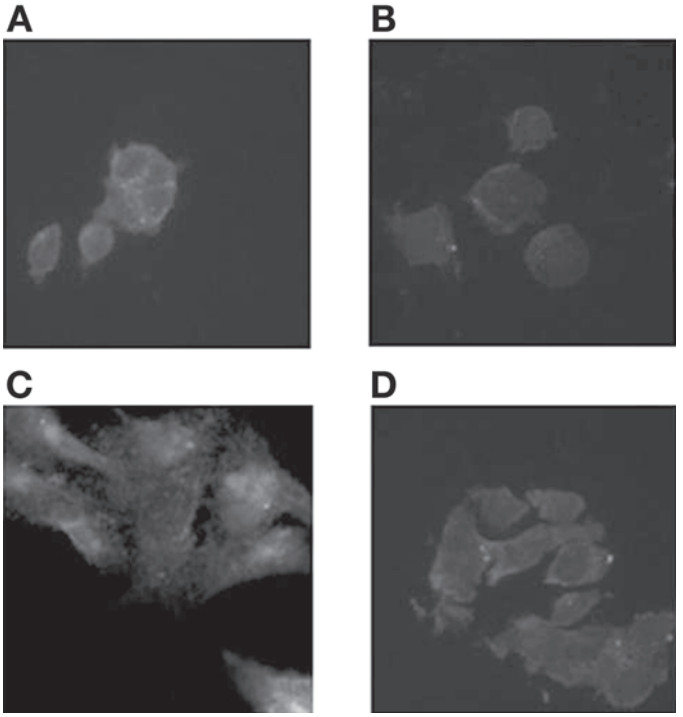

Fig. 6. H2AX staining for initiation of DNA repair in SHSY-5Y cells. SHSY-5Y cells were radiated with 20 mgy of IR as described. Cells were stained for H2AX phosphorylation **(B)** 3, **(C)** 6, and **(D)** 24 h following radiation. **(A)** NHF cells that were stained and not radiated. Pictures were taken at ×600 magnification using a confocal microscope. Initiation of DNA repair is evident in cells with brightly stained nuclear foci.

DNA Damage and Repair Induced by Radiation in NHF and SHSY-5Y Cells: H2AX Staining and Comet Assay

H2AX staining was used to indicate whether or not DNA repair processes had been activated by radiation. At three and 6 h after radiation, SHSY-5Y cells did not appear to have foci present (Fig. 6B,C), whereas NHF cells had many foci (Fig.7B,C) in comparison with control cells (Figs. 6A and 7A, respectively). These foci indicate that DNA repair processes were activated in NHF cells 1 h after radiation, whereas after the same treatment SHSY-5Y cells did not activate the DNA repair processes. After 24 h, no foci were present in either the SHSY-5Y (Fig. 6D) or NHF (Fig. 7D) cells, which indicates that DNA repair processes were no longer active in the NHF cells.

A comet assay was used to evaluate the extent of DNA damage in both cell lines. One hour after radiation very faint comet-like images were visible in the SHSY-5Y cells (Fig. 8B) and NHF cells (Fig. 9B), indicating that small amounts of DNA damage were present in both cell lines. Twenty-four hours after radiation, all the SHSY-5Y cells appeared as comet-like images

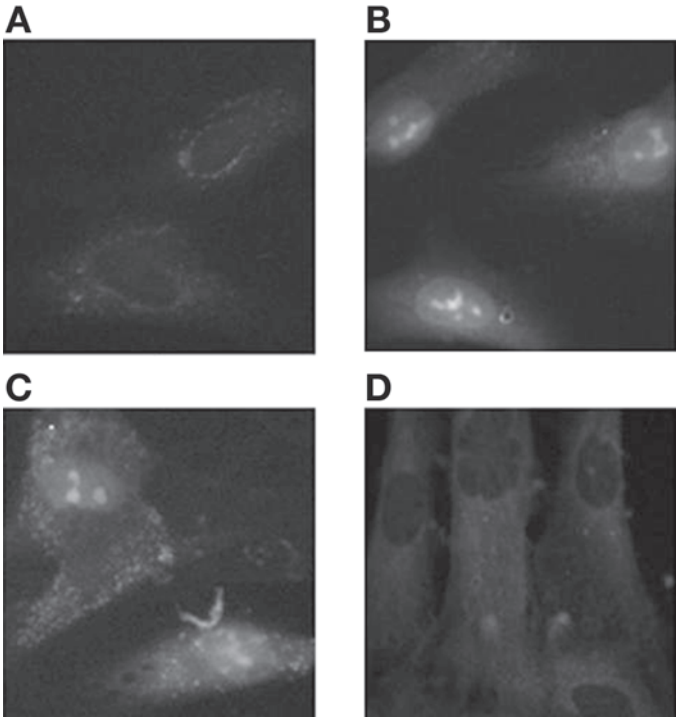

Fig. 7. H2AX staining for initiation of DNA repair in NHF cells. NHF cells were radiated with 20 mgy of IR as described. Cells were stained for H2AX phosphorylation **(B)** 3 , **(C)** 6 , and **(D)** 24 h following radiation. **(A)** NHF cells that were stained and not radiated. Pictures were taken at ×600 magnification using a confocal microscope. Initiation of DNA repair is evident in cells with brightly stained nuclear foci.

(Fig. 8C), whereas there were no visible comet-like images in the NHF cells (Fig. 9C). These results indicate that the SHSY-5Y cells had extensive DNA damage 24 h after radiation and that the small amount of DNA damage in the NHF cells was repaired.

Generation of ROS in Radiated NHF and SHSY-5Y Cells

To determine the amount of oxidative stress produced following radiation, the relative amount of ROS was measured. One hour after radiation, both NHF and SHSY-5Y cells showed increases in the amount of ROS (Fig. 10). Twenty-four hours after radiation, however, the amount of ROS decreased in the NHF cells (Fig. 10), whereas the ROS in the SHSY-5Y cells continued to climb (Fig. 10). ANOVA indicated that the control NHF ROS generation values were not significantly different from 24-h NHF ROS generation values ($p > 0.05$). ANOVA also indicated that the control SHSY-5Y and 24-h values were significantly different ($p = 0.0089$).

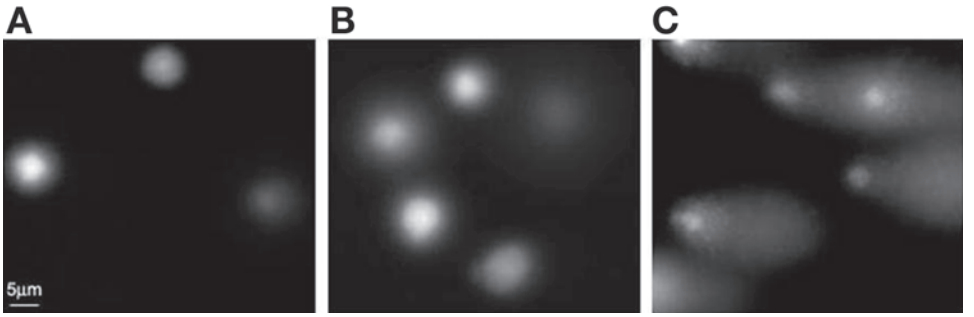

Fig. 8. Comet assay for DNA degradation: SHSY-5Y cells. SHSY-5Y cells were radiated with 20 mgy of IR as described. A comet assay was completed **(B)** 1 and **(C)** 24 h after radiation. **(A)** SHSY-5Y cells that were not radiated. Cells were stained with Hoechst 33342 dye and pictures were taken at ×400 magnification using a Leica DM IRB microscope. DNA degradation is indicated by comet-like images owing to migration of damaged DNA during electrophoresis.

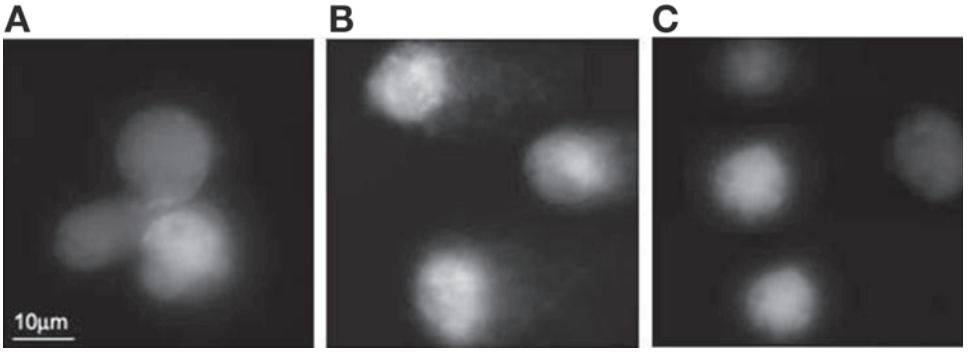

Fig. 9. Comet assay for DNA degradation: NHF cells. NHF cells were radiated with 20 mgy of IR as described. A comet assay was completed **(B)** 1 and **(C)** 24 h after radiation. **(A)** NHF cells that were not radiated. Cells were stained with Hoechst 33342 dye and pictures were taken at ×400 magnification using a Leica DM IRB microscope. DNA degradation is indicated by comet-like images owing to migration of damaged DNA during electrophoresis.

Protease Activity Induced by Radiation in NHF and SHSY-5Y Cells: Caspase-3 and Proteasome Assays

Proteases such as caspase-3 and proteasome are activated specifically as apoptosis is induced in a cell. SHSY-5Y and NHF cells were radiated and cytoplasmic extracts were used for both the caspase-3 and proteasome assays. As depicted in Fig. 11, 1 h after radiation caspase-3 activity showed slight increases in the NHF cells, but decreases close to the level of control cells 24 h after radiation. SHSY-5Y cells, on the other hand, showed an increase after 1 h and a dramatic increase after 24 h (Fig. 11). ANOVA indicated that the control NHF caspase-3 activity values were not signifi-

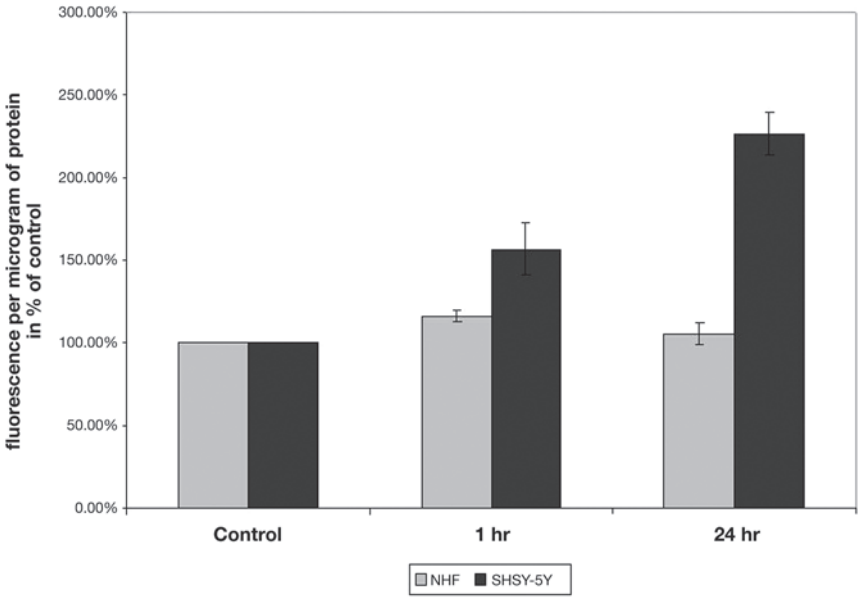

Fig. 10. Generation of ROS: NHF and SHSY-5Y. One and 24 h after radiation, DCFDA was used to measure the total cell ROS generation in NHF (shaded bars) and SHSY-5Y (black bars) cells as previously described. Microsoft Excel Version 6.0 software was used to represent the data and calculate the SD. Results were calculated per microgram of protein and SEs were calculated using data from three separate sets of experiments.

cantly different from 24-h NHF caspase-3 activity values ($p > 0.05$). ANOVA also indicated that the control SHSY-5Y and 24-h values were significantly different ($p = 0.0050$).

Proteasome activity followed a pattern similar pattern to that of caspase-3 activity. An increase in proteasome activity was observed 1 h after radiation in NHF cells but fell close to the level of the control after 24 h (Fig. 12). SHSY-5Y cells had increased proteasome activity after 1 h and a dramatic increase after 24 h (Fig. 12). ANOVA indicated that the control NHF proteasome activity values were not significantly different from 24-h NHF proteasome values ($p > 0.05$). ANOVA also indicated that the control SHSY-5Y and 24-h values were significantly different ($p = 0.0013$). Hence, the levels of apoptotic proteases in SHSY-5Y cells were indicative that apoptosis was being induced within 24 h after radiation.

Mitochondrial Changes Induced by Radiation in NHF and SHSY-5Y Cells: Membrane Permeabilization and ATP Assay

Mitochondrial membrane potential was measured as an indicator of apoptosis. SHSY-5Y and NHF cells were radiated and JC-1 and Hoechst assays were carried out as previously described. Red pigmented staining (rhodamine) is indicative of intact healthy mitochondria. Three and 6 h

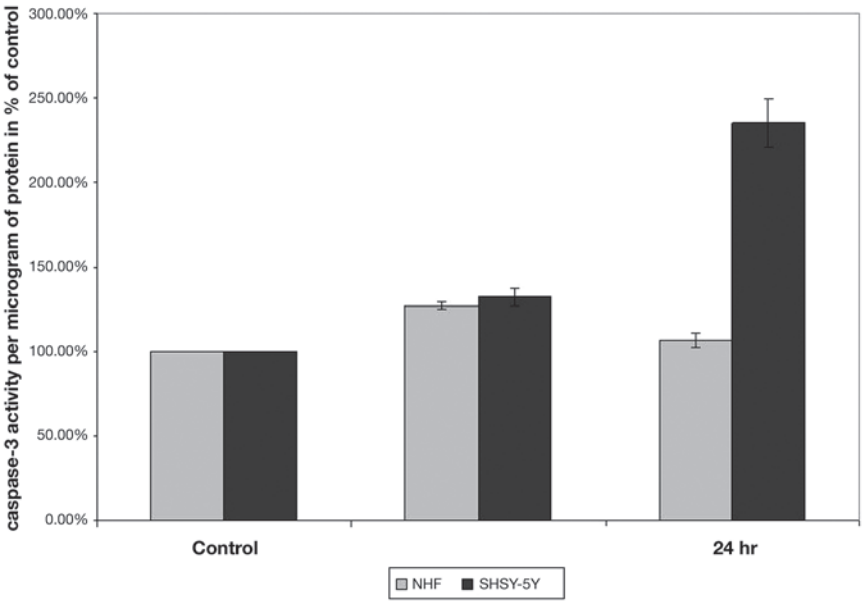

Fig. 11. Caspase-3 activity: NHF and SHSY-5Y. One and 24 h after radiation, a caspase-3 assay was used to measure caspase-3 activity in NHF (shaded bars) and SHSY-5Y (black bars) cells as previously described. Microsoft Excel Version 6.0 software was used to represent the data and calculate the SD. Results were calculated per microgram of protein and SEs were calculated using data from three separate sets of experiments.

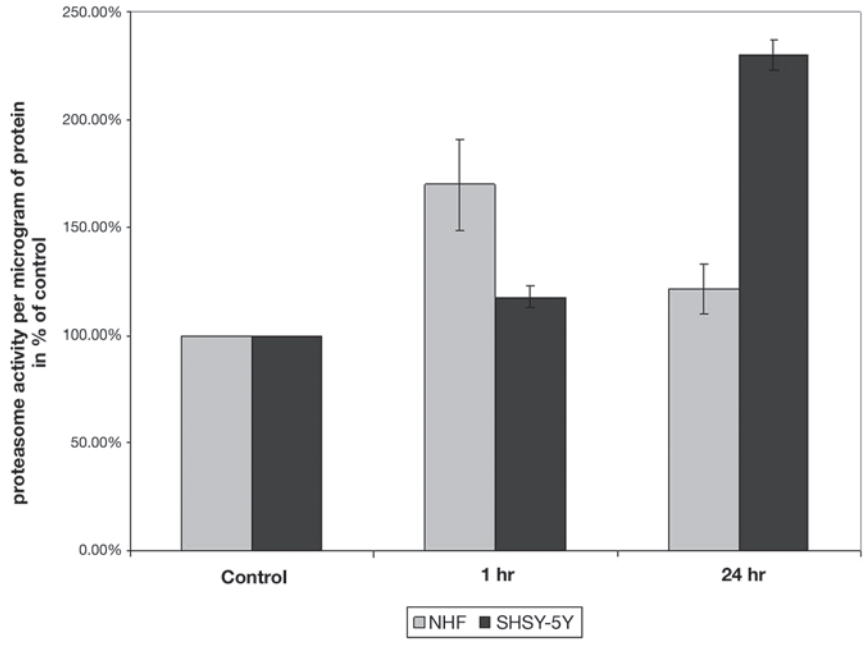

Fig. 12. Proteasome activity: NHF and SHSY-5Y. One and 24 h after radiation, a proteasome activity assay was conducted to measure the proteasome activity in NHF (shaded bars) and SHSY-5Y (black bars) cells as previously described. Microsoft Excel Version 6.0 software was used to represent the data and calculate the SD. Results were calculated per microgram of protein and SEs were calculated using data from three separate sets of experiments.

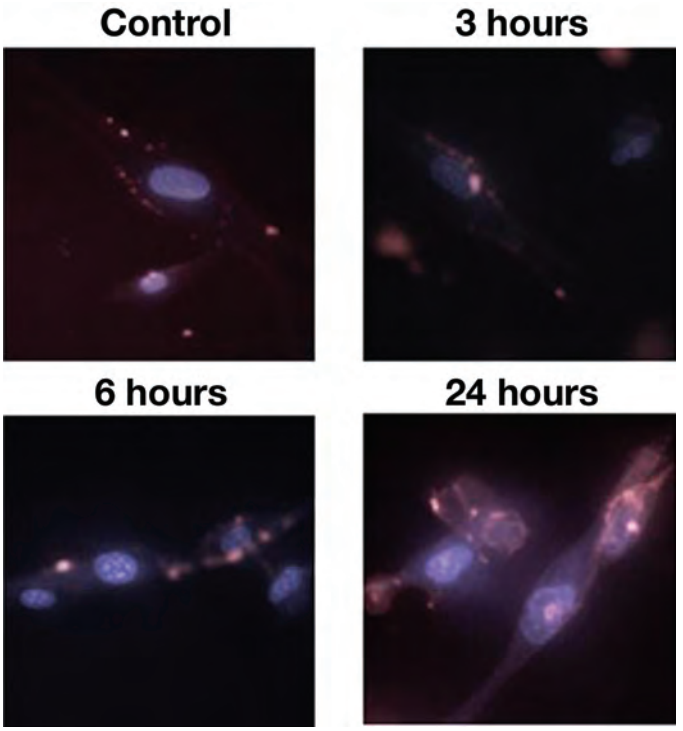
Control
3 hours
6 hours
24 hours

Fig. 13.

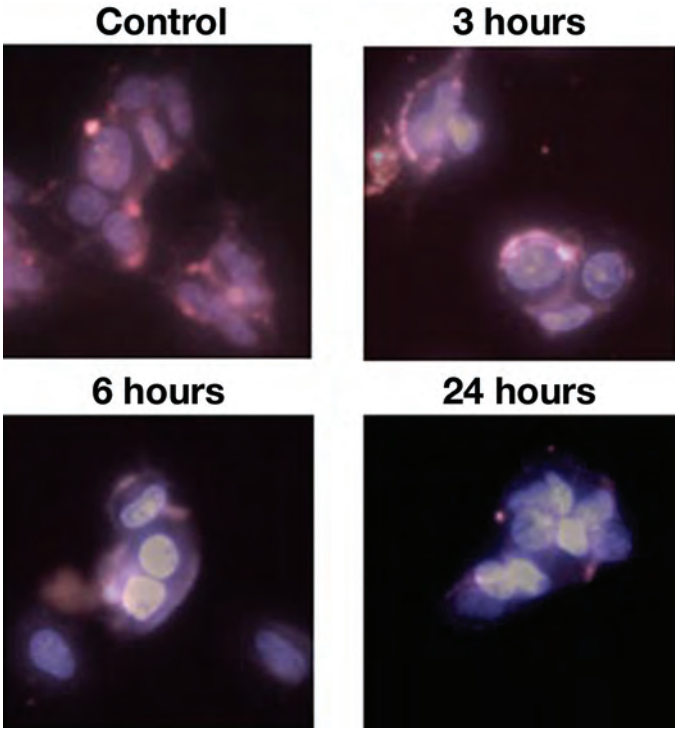
Control
3 hours
6 hours
24 hours

Fig. 14.

after the cells were irradiated, NHF cells showed no change in the mitochondrial membrane potential (Fig. 13) and appeared the same as the control cells (Fig. 13). SHSY-5Y cells did show some loss in the mitochondrial membrane potential 3 and 6 h after radiation (Fig. 14) in comparison with control cells (Fig. 14). Twenty-four hours after radiation, NHF cells clearly showed no loss in mitochondrial membrane potential (Fig. 13), whereas SHSY-5Y cells showed a nearly complete loss (Fig. 14).

SHSY-5Y and NHF cells were radiated and the cytoplasmic extracts were used to conduct an ATP assay. One hour after radiation, the total amount of ATP in both the SHSY-5Y and NHF cells decreased with respect to the control (Fig. 15). Twenty-four hours after being radiated, the SHSY-5Y cells had an even lower concentration of ATP, whereas the NHF cells regained an ATP concentration similar to that of the control (Fig. 15). ANOVA indicated that the control NHF ATP values were not significantly different from 24-h NHF ATP values ($p > 0.05$). ANOVA also indicated that the control SHSY-5Y and 24-h values were significantly different ($p = 0.0308$). These results indicate that the NHF cells were still able to produce ATP, which is indicative of healthy mitochondria, and that the SHSY-5Y cells did not recover from the damage induced by radiation.

Discussion

In the present study, we demonstrated, for the first time, the in vitro differences in the response of NHFs and cancerous SHSY-5Y cells to low-dose radiation. The results obtained indicate that an increase in ROS and DNA damage were induced in both cell lines following low-dose radiation. The differences lie in the long-term response to the DNA damage and oxidative stress. NHF cells react by initiating a rapid DNA repair response and quenching the oxidative stress in the cell. This was made evident by the disappearance of H2AX staining and the decrease in ROS after 24 h in the normal cells. The SHSY-5Y cells, on the other hand, did not repair their DNA and did not quench the increased ROS in the cell. The lack of H2AX staining is evidence that these cells did not initiate the DNA repair

Fig. 13. *(previous page)* Mitochondrial potential: NHF cells. NHF cells were radiated with 20 mgy of IR as described. Fluorescent pictures were taken 3, 6, and 24 h following radiation. After the allotted time, JC-1 dye was applied to the cells to examine mitochondrial membrane potential. Pictures were taken at ×400 magnification using a Leica DM IRB microscope. Red pigmented staining (rhodamine) is indicative of intact healthy mitochondria.

Fig. 14. *(previous page)* Mitochondrial potential: SHSY-5Y cells. SHSY-5Y cells were radiated with 20 mgy of IR as described. Fluorescent pictures were taken 3, 6, and 24 h following radiation. After the allotted time, JC-1 dye was applied to the cells to examine mitochondrial membrane potential. Pictures were taken at ×400 magnification using a Leica DM IRB microscope. Red staining (rhodamine) is indicative of intact healthy mitochondria.

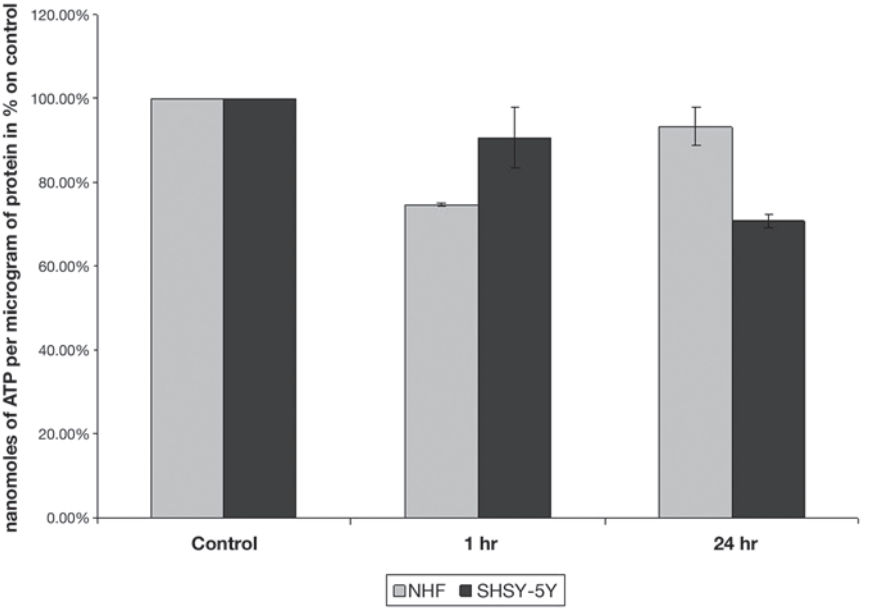

Fig. 15. Generation of ATP: NHF and SHSY-5Y. One and 24 h after radiation, an ATP assay was conducted in order to estimate the amount of ATP in the SHSY-5Y (black bars) and NHF (shaded bars) cells as previously described. Microsoft Excel Version 6.0 software was used to represent the data and calculate the SD. Results were calculated per microgram of protein and SEs were calculated using data from three separate sets of experiments.

mechanism observed in the normal cell line. In fact, SHSY-5Y cells showed characteristic signs that they were beginning to undergo apoptosis.

Past studies have found that activation of the DNA repair response by phosphorylation of the H2AX molecules flanking the DSB is a relatively quick response *(22)*. In the present study, H2AX staining functioned as a sensitive technique for the examination of DSB and repair induced by radiation *(14)*.

SHSY-5Y cells showed a significant increase in the activity of proteases and an increase in the number of cells with apoptotic morphologic characteristics such as nuclear condensation. These results are consistent with past research indicating that cells begin to undergo apoptosis 24–48 h following injury to the DNA *(23)*. NHF cells did not show any of these classic signs of apoptosis and appeared to have lower levels of proteases, a higher percentage of viable cells, and a lack of apoptotic morphologic characteristics similar to those seen in the control cells.

Recent studies have reported that each focus visualized by H2AX staining is representative of an individual break, and, thus, the lack of foci would appear to represent the repair of the DSBs owing to this one-to-one ratio *(12)*. Other studies, however, have found that a decrease in the number of cells with foci is not always consistent with the number of cells that have

undergone full DNA repair *(12)*. To eliminate this possibility, a comet assay was used to evaluate the extent of the DNA damage. Comet assays have been used in the past as a sensitive assay for measuring and identifying DNA damage at the cellular level *(18,24,25)*. The results of the comet assay illustrate that the SHSY-5Y cells did not seem to repair their DNA; however, since the NHF cells no longer had DNA damage after 24 h, a successful repair mechanism was in place.

The mechanism by which SHSY-5Y cells undergo apoptosis after treatment with low doses of IR is unknown. Although DNA damage *(26)* and the lack of an ability to repair DSBs can induce apoptosis, the oxidative stress generated by the immediate increase in ROS may also play a role *(27)*. Past research has found that oxidative stress induces apoptosis in many different cell lines *(28)* and that at higher doses of radiation mitochondria may be responsible for the later increase in ROS observed in a wide variety of cells *(29,30)*. The increased oxidative stress owing to higher levels of ROS in SHSY-5Y cells may lead to detrimental effects on the mitochondria by acting at the permeability transition pores and lead to collapse of the mitochondrial membrane *(31)*. Mitochondria play a key role in the apoptosis of mammalian cells *(32)*, and the findings of our study imply that permeabilization of the mitochondrial membrane may play a part in the apoptotic cell death of cancer cells after treatment with low-dose IR.

Further research into the mechanism of how cancer cells undergo apoptosis and normal cells initiate a repair mechanism is required. The present study gives insight into the possible mechanism and acts as a stepping-stone for future studies. One of the most significant findings from this study is the difference between the cellular responses to the same low-dose radiation treatment of a normal and a cancerous cell line: low-dose radiation appears to be tolerated in normal cells, whereas SHSY-5Y cells begin to undergo apoptosis. Two main types of stress occur in both types of cells following low-dose radiation: oxidative stress caused by an increase in ROS, and DNA DSBs directly or indirectly caused by the exposure to radiation. Why, then, do the cancer cells undergo apoptosis whereas the normal cells are able to deal with the stress? The answer is not yet quite clear.

Cancer cells divide at an extremely fast rate and, thus, may not take the time to properly prepare every component of the cell for division. As a result, it is possible for cells to have weaker mitochondria that are unable to survive additional oxidative stress caused by the increase in ROS. Past research has found that there may be some differences between the mitochondria of cancer and normal cells *(33)*. The increase in oxidative stress may cause the loss of the mitochondria membrane potential in SHSY-5Y cells following radiation and, thus, the mitochondria may be the starting point of the apoptotic mechanism. Normal cells also seem to be better equipped to deal with the oxidative stress caused by an increase in ROS.

Our study has provided novel insight into the differences between SHSY-5Y and NHF cells in their response to DNA damage and increased ROS following a low dose of radiation. Further study is needed to elucidate

the mechanism by which SHSY-5Y cells undergo apoptosis following radiation and why the normal cells are better equipped to deal with the additional oxidative stress and numerous DSBs. This study has opened the doors for further study into the differences between normal and cancer cells, which will provide new insight for possible ways to combat cancer and leave patients relatively free of the current side effects. These treatments may be a form of low-dose radiation or a novel treatment that will prey on these differences in order to selectively kill cancer.

Acknowledgments

We gratefully acknowledge Natasha Kekre for help in conducting the comet assay, Natasha Sharda for help with the H2AX staining, and Sapal Bonny for help in radiating the cells. This work was supported by grants from the Canadian Foundation for Innovation, Ontario Innovation Trust, and the Natural Sciences and Engineering Research Council. Further thanks are due the Windsor Regional Cancer Centre and Dr. Huston for the use of their facilities.

References

1. Martin, N. M. B. (2001), *J. Photochem. Photobiol. B* **63,** 162–170.
2. Saint John's Health Center (www.stjohns.org), Santa Monica, CA: St. John's Health Center; 1999 (accessed June 15, 2004). What is radiation therapy? Available from: www.stjohns.org/our_health_services/oncology_what.asp.
3. Jeremic, B. (2004), *Hematol. Oncol. Clin. North Am.* **18,** 1–12.
4. Shinomiya, N. (2001), *J. Cell. Mol. Med*. **5,** 240–253.
5. Zhang, M., Stevens, G., and Madigan, C. (2001), *Int. J. Cancer* **96(Suppl.),** 7–14.
6. Jiang, Y. L., Escano, M. F. T., Sasaki, R., et al. (2004), *Jpn. J. Ophthalmol.* **48,** 106–114.
7. Pandey, S., Smith, B., Walker, P. R., and Sikorska, M. (2000), *Apoptosis* **5,** 265–275.
8. Green, D. R. and Reed, J. C. (1998), *Science* **281,** 1309–1312.
9. Hickey, E. J., Raje, R. R., Reid, V. E., et al. (2001), *Free Radic. Biol. Med.* **31,** 139–152.
10. Hui, W. and Kavanagh, J. J. (2003), *Lancet Oncol*. **4,** 721–729.
11. Janicke, R. U., Engels, I. H., Dunkern, T., Kaina, B., Schulze-Osthoff, K., and Porter, A. G. (2001), *Oncogene* **20,** 5043–5053.
12. Rothkamm, K. and Löbrich, M. (2003), *Proc. Natl. Acad. Sci. USA* **9,** 5057–5062.
13. Banath, J. P. and Olive, P. L. (2003), *Cancer Res*. **63,** 4347–4350.
14. MacPhail, S. H., Banath, J. P., Yu, T. Y., Chu, E. H., Lambur, H., and Olive, P. L. (2003), *Int. J. Radiat. Biol*. **79,** 351–358.
15. Shiloh, Y. (2001), *Curr. Opin. Genet. Dev*. **11,** 71–77.
16. Bassing, C., Chua, K. F., Sekiguchi, J., et al. (2002), *Proc. Natl. Acad. Sci. USA* **99,** 8173–8178.
17. Limoli, C. L., Giedzinski, E., Bonner, W., and Cleaver, J. E. (2002), *Proc. Natl. Acad. Sci. USA* **99,** 233–238.
18. Hook, G., Zhang, P., Lagroye, I., et al. (2004), *Radiat. Res.* **161,** 193–200.
19. Naderi, J., Hung, M., and Pandey, S. (2003), *Apoptosis* **8,** 91–100.
20. Siraki, A. G., Pourahmad, J., Chan, T. S., Khon, S., and O'Brien, P. J. (2002), *Free Radic. Biol. Med*. **32,** 2–10.
21. Olichon, A., Baricault, L., Gas, N., et al. (2003), *J. Biol. Chem.* **278,** 7743–7746.
22. Huang, X., Okafuki, M., Traganos, F., Luther, E., Holden, E., and Darzykiewicz, Z. (2004), *Cytometry* **58A,** 99–110.
23. Brown, J. M. and Wilson, G. (2003), *Cancer Biol. Ther*. **2,** 477–490.

24. Bacova, G., Hunakova, L. E., Chorvath, M., et al. (2000), *Neoplasma* **47,** 367–374.
25. Dunn, A. L., Price, M. E., Mothersill, C., McKeown, S. R., Robson, T., and Hirst, D. G. (2003), *Br. J. Cancer* **89,** 2277–2283.
26. Chan, W. H. and Yu, J. S. (2000), *J. Cell Biochem.* **78,** 73–84.
27. Lai, H. and Singh, N. P. (2004), *Environ. Health Perspect.* **6,** 687–694.
28. Chun, H. S., Gibson, G. E., DeGiorgio, L. A., Zhang, H., Kidd, V. J., and Son, J. H. (2001), *J. Neurochem.* **76,** 1010–1021.
29. Leach, K., Tuyle, G. V., Lin, P., Schmidt-Ullrich, R., and Mikkelsen, R. B. (2001), *Cancer Res.* **61,** 3894–3901.
30. Llagostera, E., Soto-Cerrato, V., Montaner, B., and Perez-Tomas, R. (2003), *Ann. N Y Acad. Sci.* **1010,** 178–181.
31. Piret, J. P., Arnould, T., Fuks, B., Chatelain, P., Remacle, J., and Michiels, C. (2004), *Biochem. Pharmacol*. **67,** 611–620.
32. McCarthy, S., Somayajulu, M., Sikorska, M., Borowy-Borowski, H., and Pandey, S. (2004), *Toxicol. Appl. Pharmacol.*, **201,** 21–31.
33. Villa, A. M. and Doglia, S. M. (2004), *J. Biomed. Opt*. **9,** 385–394.